

# Enhanced visible light photocatalytic activity of SDBS/C/Nd/TiO<sub>2</sub> synthesized by using anionic surfactant SDBS as template agent

Dandan Wang<sup>1,2</sup>, Yuan Yuan<sup>2</sup>, Mengli Wang<sup>2</sup>, Tao Bi<sup>2</sup>, Chao Li<sup>2,\*</sup> and Lin Zhao<sup>1</sup>

<sup>1</sup>College of Environmental Science and Engineering, Tianjin University, Tianjin, China

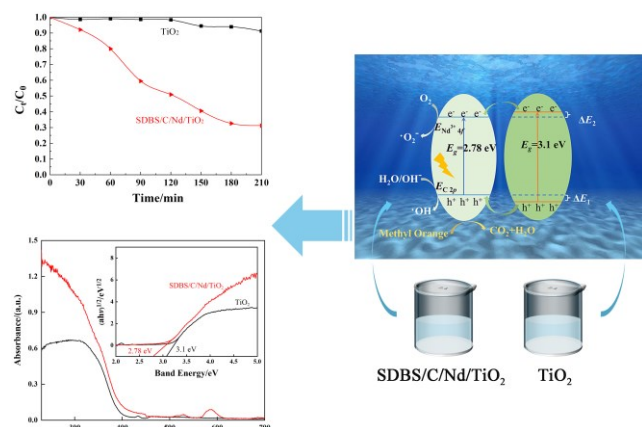
<sup>2</sup>Huace Eco Environmental Technology (Tianjin) Co., Ltd, Tianjin, China

Received: 10/01/2024, Accepted: 29/05/2024, Available online: 20/06/2024

\*to whom all correspondence should be addressed: e-mail: lichao0618@163.com

<https://doi.org/10.30955/gnj.05718>

## Graphical abstract



## Abstract

The catalyst SDBS/C/Nd/TiO<sub>2</sub> was synthesized by sol-gel method using TiO<sub>2</sub> co-doped with C and Nd and anionic surfactant SDBS as template agent. The prepared photocatalysts were characterized by X-ray diffraction (XRD), scanning electron (SEM), X-ray photoelectron spectrometer (XPS) and UV-vis diffuse reflectance spectroscopy (UV-vis DRS) and so on. Experimental results show that the crystal structure of the catalytic material is anatase type. Since doped elements change the energy band structure and electronic structure of TiO<sub>2</sub>, photogenerated electrons and holes can transition through the intermediate energy level, resulting in a decrease in the required excitation energy, thereby increasing the distance of its absorption edge moving toward the long wave direction, and meanwhile improving the utilization rate of visible light. The bandgap energy of the catalyst SDBS/C/Nd/TiO<sub>2</sub> was 2.78 eV. Compared to pure TiO<sub>2</sub> (3.1 eV), the band gap is reduced by 0.32 eV. The photocatalytic experiments show that the degradation rate of the catalyst SDBS/C/Nd/TiO<sub>2</sub> for methyl orange solution can reach 67%, and the catalytic performance is much improved than that of pure TiO<sub>2</sub>.

**Keywords:** Sol-gel method, anionic surfactant, catalytic material, energy level, catalytic performance

## 1. Introduction

The excessive manipulation and use of resources and the deep pollution of nature pose a certain threat to the environment on which human beings depend for survival. Photocatalysis has shown a wide application prospect in the field of remediation of environmental pollution, thus making this technology receive wide attention and become a hot spot of current research (Xie *et al.* 2014; Sudarsanam *et al.* 2020; Xia *et al.* 2023). In general, the photocatalytic materials have many advantages, such as the low toxicity, cheap cost, mild conditions, good chemical stability and strong oxidation ability (Yu *et al.* 2017; Krylov *et al.* 2021), but they only have certain absorption performance under the condition of ultraviolet light, which results in the decrease of solar energy utilization (Xiao *et al.* 2016). This is one of the disadvantages that has been restricting the improvement of photocatalytic activity. Therefore, how to modify the photocatalytic materials and extend the field of light response to the visible region, so that it can be applied to real production and life, has become the focus of in-depth research (Kuerbanjiang *et al.* 2013).

A more promising photocatalyst under current conditions is TiO<sub>2</sub> (Verbruggen, 2015). In order to improve the photocatalytic efficiency of TiO<sub>2</sub> in the visible light range, people has adopted a series of measures, such as: heterostructure (Liu *et al.* 2012), dye sensitized (Zhao *et al.* 2023) and ions doped (Yin *et al.* 2005; Dwiyantha *et al.* 2021), in which the ions doped is an easy operation and effective method. The ions doped include nonmetal, metal ion, inert metal and rare earth metal doped (Kader *et al.* 2022; Kunarti *et al.* 2020; Jin *et al.* 2023; Vishwakarma *et al.* 2023). The co-doped of two or more ions can significantly improve the photocatalytic activity due to the synergistic effect of ions (Sirivallop *et al.* 2020; Wang *et al.* 2022; Chen *et al.* 2017). Among them, the rare earth metal ions have an unfilled 4f layer for transition. Due to such special structure, they are of great help to expand the range of absorption spectrum, more and more scholars have studied them, in which Nd element has received a lot of attentions as the rare earth element.

Rengaraj (Rengaraj *et al.* 2007) pointed out that Nd doped TiO<sub>2</sub> can capture electron centers, provide more charge carriers and effectively separate electrons and holes on the surface of TiO<sub>2</sub> through redox reaction. After decades of research and development, semiconductor photocatalytic technology has been applied in the fields of solar energy utilization, environmental improvement and medical health (Chen *et al.* 2010), but still has some problems: such as, the narrow spectral response and the low quantum efficiency result in a certain distance in its industrial production.

In the process of material synthesis, the addition of surfactant plays an important role in regulating the morphology of catalyst. Sodium dodecyl benzene sulfonate (SDBS) is a multifunctional chemical whose applications cover many different fields. Its surface activity and dispersion ability make it one of the indispensable ingredients in a variety of products and industrial processes. Whether used in detergent manufacturing, pharmaceutical preparations, laboratory research or other industrial applications, SDBS plays an important role. In addition, SDBS can also be used as a structure-oriented agent when crystal growth is performed by hydrothermal or solvothermal methods. At the same time, the morphology and particle size of the material can be changed by controlling the amount of SDBS (Zhang *et al.* 2023; Si *et al.* 2018).

In this paper, SDBS/C/Nd/TiO<sub>2</sub> catalyst was designed and synthesized by sol-gel method (Marzec *et al.* 2016; Li *et al.* 2015) using SDBS as template agent. By adding the anionic surfactant SDBS, the particle size of the catalyst can be uniformly dispersed, the particle size is consistent, and the specific surface area and pore size of the catalyst can be expanded. The photocatalytic properties of the prepared catalysts were tested with methyl orange solution as the probe, and the photocatalytic mechanism was studied by combining experiment results. The results show that the prepared SDBS/C/Nd/TiO<sub>2</sub> achieves a significant enhancement in photocatalytic performance compared with the pure TiO<sub>2</sub>.

## 2. Materials and methods

### 2.1. Materials

Butyl titanate (AR, 98%) and glucose (AR, 98%) were obtained from Tianjin Kemi Ou Chemical Reagent Co., LTD, sodium dodecyl benzoate (AR, 90%) was obtained from Zhengzhou Yongxing Chemical Co., LTD, anhydrous ethanol (AR, 75%), neodymium nitrate (AR, 99%), glacial acetic acid (AR, 36%) and nitric acid (AR, 65%-68%) were obtained from Tianjin Kaitong Chemical reagent Co., LTD.

### 2.2. Synthesis

#### 2.2.1. TiO<sub>2</sub> catalyst

TiO<sub>2</sub> catalyst was synthesized by sol-gel method. Firstly, a certain volume of butyl titanate was measured and added to anhydrous ethanol, then, the mixture was stirred for 30 minutes, denoted as liquid A. A certain volume of distilled water and anhydrous ethanol were mixed simultaneously, and dilute nitric acid was used to adjust the pH of the

solution, denoted as liquid B. Add the B solution to the A solution drop by drop, and in a certain temperature under stirring for several hours, get wet sol, transferred to the reaction kettle in drum wind drying oven aging 2 d, decompression filtration, 100 °C vacuum drying 2 h. Thus, TiO<sub>2</sub> catalyst was successfully prepared.

#### 2.2.2. SDBS/C/Nd/TiO<sub>2</sub> catalyst

SDBS/C/Nd/TiO<sub>2</sub> catalyst was prepared by sol-gel method using SDBS as template. A certain volume of butyl titanate was measured and added to anhydrous ethanol, then, the mixture was stirred for 30 minutes, denoted as liquid A. Anhydrous ethanol, deionized water, glacial acetic acid, glucose, Nd(NO<sub>3</sub>)<sub>3</sub> and SDBS were measured and added into the beaker to dissolve and dilute nitric acid was used to adjust the pH of the solution, denoted as liquid B. Add the B solution to the A solution drop by drop, and in a certain temperature under stirring for several hours, get wet sol, transferred to the reaction kettle in drum wind drying oven aging 2 d, decompression filtration, 100 °C vacuum drying 2 h. Subsequently, the SDBS/C/Nd/TiO<sub>2</sub> catalyst could be obtained.

### 2.3. Characterization

A Japanese HITACHI s-4300 scanning electron microscopy and Japanese H-7650 transmission electron microscopy were used to observe the catalysts in terms of their dispersion, morphology and particle size; a D8-FOCUS X-ray diffractometer from Germany was used to test the crystal structure; X-ray photoelectron spectroscopy of ESCALAB250Xi from Thermo, USA was used to explore the classification of material elements, the combination of elements and their percentages; the characteristics of absorption peaks were used for qualitative analysis by the TU-1901 UV-visible diffuse reflection; the N<sub>2</sub> adsorption-desorption of the catalysts were measured by Quntachrome Nova Win2 physical adsorption instrument of konta and the specific surfaces and pore volumes of the catalysts were calculated by BET and BJH.

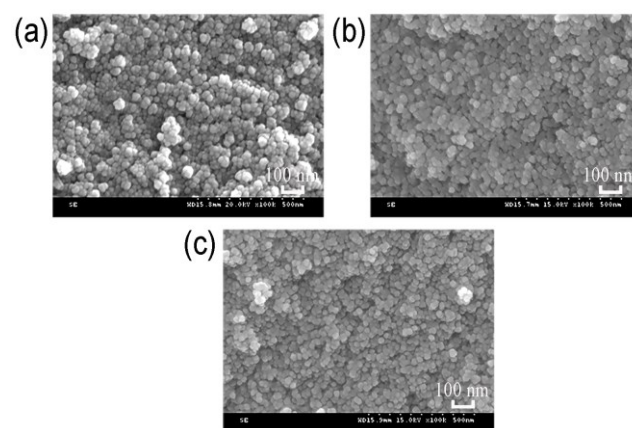


**Figure 1.** SEM of a) TiO<sub>2</sub>, b) SDBS and c) SDBS/C/Nd/TiO<sub>2</sub>

### 2.4. Photocatalytic performance

Photocatalytic experiments were carried out by using 1000 W xenon lamp as the simulating light source and using methyl orange solution as the probe. 50 mL of the dye solution was added in the test tube, and 0.1g of different catalysts were weighed in the above solution, respectively, which was put into the light reaction and

stirred for 30 minutes closing the light, the sample was denoted as 0 min. Open the light, and the sample was taken every 30 min. The TU1901 UV-visible spectrophotometer was used to test the absorbance. The decolorization rate was calculated by formula 1, and the performance of dye degradation was compared :

$$\eta = \frac{A_0 - A_t}{A_0} \times 100\% \quad (1)$$

Formula 1 represents the formula of decolorization rate, where  $A_0$  represents the absorbance of the dye solution after being stirred for 30 minutes in the dark;  $A_t$  is the absorbance of the solution light t min.

### 3. Results and discussion

#### 3.1. Morphology of catalyst

Scanning electron microscopy (SEM) was used to analyze the morphology of the samples. The SEM images of TiO<sub>2</sub>, SDBS and SDBS/C/Nd/TiO<sub>2</sub> are shown in Figure 1a-1c, respectively. It could be seen that all three samples are composed of spherical particles. It is obvious that the

addition of anionic surfactant SBDS is conducive to the same surface particle size and uniform dispersion. Compared with pure TiO<sub>2</sub>, the surface morphology of TiO<sub>2</sub> was improved by using sodium dodecyl sulfate as a surfactant.

#### 3.2. X-ray diffractometer

The XRD patterns of TiO<sub>2</sub> and SDBS/C/Nd/TiO<sub>2</sub> were shown in Figure 2a. By comparing the standard JCPDF cards, it is obvious that all the strong patterns are in agreement with the pure anatase-type TiO<sub>2</sub>. At the same time, no other impurity diffraction peaks appeared, which clearly demonstrate the phase purity.

**Table 1.** The information for the samples TiO<sub>2</sub> and SDBS/C/Nd/TiO<sub>2</sub>

Samples	TiO <sub>2</sub>	SDBS/C/Nd/TiO <sub>2</sub>
Band gap/eV	3.10	2.78
Specific surface area/m <sup>2</sup> g <sup>-1</sup>	55.22	116.1
Pore volume/cm <sup>3</sup> g <sup>-1</sup>	0.089	0.361

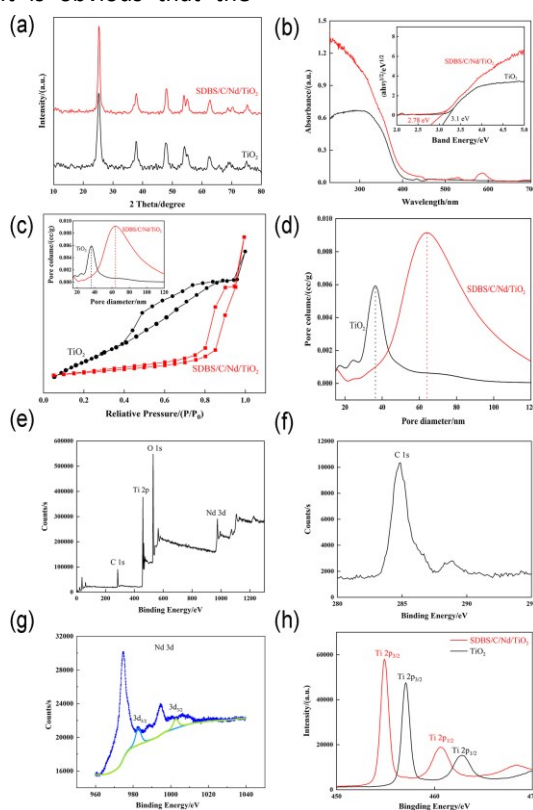


**Figure 2.** a) XRD spectrum of TiO<sub>2</sub> and SDBS/C/Nd/TiO<sub>2</sub>; b) UV-vis-NIR diffuse reflectance spectrum of TiO<sub>2</sub> and SDBS/C/Nd/TiO<sub>2</sub>; c) and d) the N<sub>2</sub> adsorption - desorption isotherm and pore size distribution of TiO<sub>2</sub> and SDBS/C/Nd/TiO<sub>2</sub>; e) - f) XPS spectra of TiO<sub>2</sub> and SDBS/C/Nd/TiO<sub>2</sub>

#### 3.3. UV-vis-NIR diffuse reflectance spectroscopy

As can be seen from Figure 2b, absorption in the wavelength range less than 400 nm is obviously determined by the inherent absorption characteristics of TiO<sub>2</sub> and the absorption edge of SDBS/C/Nd/TiO<sub>2</sub> catalyst moves towards the long wave direction. Therefore, the band gap of TiO<sub>2</sub> and SDBS/C/Nd/TiO<sub>2</sub> is 3.1eV and 2.78eV, respectively (as shown in Table 1). The absorption performance of SDBS/C/Nd/TiO<sub>2</sub> in the ultraviolet region

is enhanced compared with pure TiO<sub>2</sub>. This shows that the adding of anionic surfactant and the doping of elements change the absorption performance of TiO<sub>2</sub>, which makes the catalyst SDBS/C/Nd/TiO<sub>2</sub> have higher absorption in the ultraviolet region. Two absorption peaks appear at the wavelength of 550 and 590 nm, which is a unique property of Nd element, thus demonstrating that Nd<sup>3+</sup> ions are successfully doped into the catalyst. Because the doped element changes its internal energy band structure



and electronic structure, intermediate energy levels may be generated between the valence band and conduction band of  $\text{TiO}_2$ , and photogenerated electrons and holes can transition through these intermediate energy levels. The required excitation energy is reduced to the visible light range, so that doped  $\text{TiO}_2$  has visible light absorption and absorption energy. Thus, it is beneficial to improve the utilization rate of visible light.

### 3.4. $\text{N}_2$ adsorption-desorption

Figure 2c shows that the relative pressure range is 0.8-1, and both catalysts have a hysteresis ring, indicating that both catalysts have pore structures. The specific surface area, pore volume and pore diameter of different catalytic materials can be obtained by BET model and BJH model. According to the classification of BDDT, the  $\text{N}_2$  adsorption-desorption isotherm of the prepared catalytic material belongs to type IV. It can be seen from Figure 2d the pore size distribution curve that the pore size of  $\text{TiO}_2$  and SDBS/C/Nd/ $\text{TiO}_2$  catalytic materials is concentrated between 30 nm and 50 nm, which belongs to mesoporous materials. The specific surface area and pore volume of  $\text{TiO}_2$  and SDBS/C/Nd/ $\text{TiO}_2$  are  $55.22 \text{ m}^2\text{g}^{-1}$  and  $0.089 \text{ cm}^3\text{g}^{-1}$  and  $116.1 \text{ m}^2\text{g}^{-1}$ ,  $0.361 \text{ cm}^3\text{g}^{-1}$ , respectively. The results are shown in Table 1. According to the data in Table 1, compared with pure  $\text{TiO}_2$ , the pore volume of SDBS/C/Nd/ $\text{TiO}_2$  is smaller than that of pure  $\text{TiO}_2$ , and the corresponding specific surface area is larger than that of pure  $\text{TiO}_2$ , which indicates that the specific surface area of the catalytic material can be improved to a certain extent after adding anionic surfactants and doping with elements. Such a large specific surface area and porous structure for SDBS/C/Nd/ $\text{TiO}_2$  are conducive to the rapid diffusion of reactants and products, thus promoting the improvement of photocatalytic activity. The large pore volume provides a good mass transfer space for dynamic reactants and reduces steric hindrance. It helps to speed up the reaction rate. Thus, SDBS/C/Nd/ $\text{TiO}_2$  catalytic material has higher photocatalytic activity.

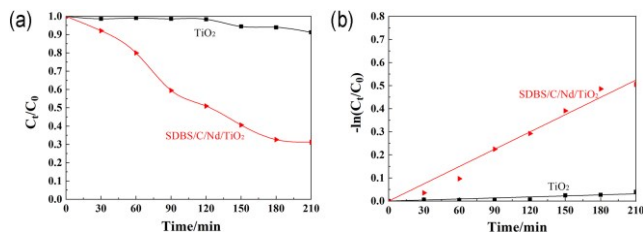
### 3.5. X-ray photoelectron spectroscopy

Figure 2e-h shows the full spectrum of SDBS/C/Nd/ $\text{TiO}_2$ , C 1s spectrum, Nd 3d spectrum and Ti 2p binding energy change spectrum, respectively. As can be seen from Figure 2e, both C and Nd elements have been successfully doped into  $\text{TiO}_2$ . Combined with XPS data analysis, the characteristic peaks of C 1s, Nd 3d<sup>3</sup>, Nd 3d<sup>5</sup>, Ti 2p and O 1s are located around 288 eV, 1002 eV, 982 eV, 458.78 eV and 530 eV. Comparing with the Ti 2p binding energy of  $\text{TiO}_2$  and SDBS/C/Nd/ $\text{TiO}_2$  (Figure 2h), the orbital electron binding energy of Ti 2p of SDBS/C/Nd/ $\text{TiO}_2$  moves to the low energy region. This is due to the fact that Nd is less electronegative than Ti, which causes the electron cloud around Ti to become denser.

### 3.6. Catalytic activity

The photocatalytic activity of the catalysts in visible light was evaluated according to the decolorization rate of methyl orange solution. The results are shown in Figure 3. From Figure 3a, catalysts under the condition of visible light has a certain degradation ability, the SDBS/C/Nd/ $\text{TiO}_2$

have larger decolorization rate, which can achieve 67%, mainly because SDBS/C/Nd/ $\text{TiO}_2$  has larger specific surface area and pore volume, thus the larger mass transfer space is provided for photocatalytic and it is favorable for the improvement of photocatalytic activity.



**Figure 3.** a) The degradation of methyl orange dye by catalytic materials; b) the first order kinetic response spectra

The decolorization rate of methyl orange solution follows the first-order kinetic model, as shown in Figure.3b, which can be expressed as  $-\ln(C_t/C_0) = Kt$ , Where,  $C_0$  is the initial concentration of methyl orange solution;  $C_t$  is the concentration of light t min methyl orange solution; K is the rate constant; higher K means higher photocatalytic activity. The photocatalytic rate constant of SDBS/C/Nd/ $\text{TiO}_2$  is higher than that of  $\text{TiO}_2$  catalyst, which indicates that the photocatalytic activity of SDBS/C/Nd/ $\text{TiO}_2$  is significantly higher than that of  $\text{TiO}_2$  catalyst.

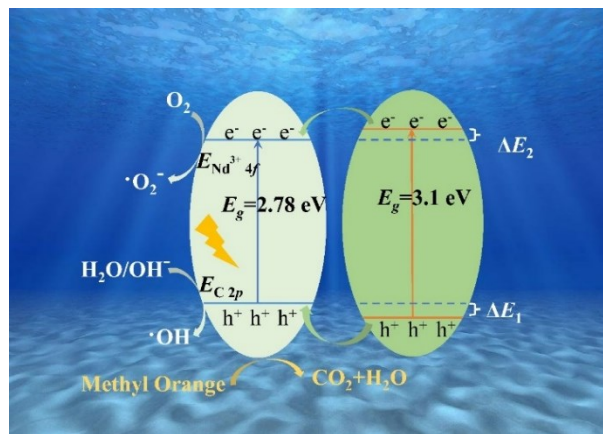


**Figure 4.** The photocatalytic possibility mechanism of SDBS/C/Nd/ $\text{TiO}_2$

### 3.7. Study on photocatalytic activity mechanism

According to the experimental characterization of SDBS/C/Nd/ $\text{TiO}_2$ , the possibility mechanism of photocatalysis of SDBS/C/Nd/ $\text{TiO}_2$  catalyst is inferred as shown in Figure 4. The synergistic effect of non-metallic C and rare earth metal Nd makes the band gap of SDBS/C/Nd/ $\text{TiO}_2$  narrower. The doping of C element with 2p empty orbital into  $\text{TiO}_2$  can produce a new energy band  $E_{C2p}$ , which is above the valence band (VB) of  $\text{TiO}_2$ . When Nd is doped in  $\text{TiO}_2$ , a new energy band  $E_{Nd^{3+} 4f}$ , which is lower than  $\text{TiO}_2$  conduction band (CB), is generated due to the empty orbital of Nd 4f, forming the energy difference  $\Delta E_1$  and  $\Delta E_2$ . Thus, the photocatalytic performance of SDBS/C/Nd/ $\text{TiO}_2$  catalyst is improved. At the same time,  $\text{O}_2$  and  $\text{H}_2\text{O}/\text{OH}^-$  adsorbed on the surface of nanoparticles capture electrons and holes, and undergo REDOX reaction to produce  $\bullet\text{O}_2^-$  and  $\bullet\text{OH}$ , oxidizing organic pollutants to  $\text{CO}_2$  and  $\text{H}_2\text{O}$ , reduces the recombination of

photogenerated electrons and holes, and is more conducive to enhancing photocatalytic activity. Sodium dodecyl sulfate, as a surfactant, improved the surface morphology of TiO<sub>2</sub> by sol-gel process and found that TiO<sub>2</sub> modified by non-metallic C and rare earth metal Nd showed higher photocatalytic efficiency. SDBS/C/Nd/TiO<sub>2</sub> photocatalyst has a wide range of applications in the environmental field, such as air purification, water treatment, and can also decompose harmful gases in the air, effectively removing pollutants in indoor air.

#### 4. Conclusion

In summary, SDBS/C/Nd/TiO<sub>2</sub> and pure TiO<sub>2</sub> catalysts were prepared by sol-gel method. According to experimental results, the morphology and crystal form of the SDBS/C/Nd/TiO<sub>2</sub> catalyst were not significantly changed, but the absorption performance of the catalyst was improved, and the specific surface area was increased after the doping of C and Nd. After using SDBS as the template agent, the surface particle dispersion of SDBS/C/Nd/TiO<sub>2</sub> is improved and the agglomeration phenomenon is reduced. The crystal type of the catalyst is still anatase after doping, and the absorption edge of light has a certain degree of red shift, which is conducive to enhancing the absorption of visible light. Based on photocatalytic experiment, the SDBS/C/Nd/TiO<sub>2</sub> degradation of methyl orange solution is higher than pure TiO<sub>2</sub>, the decolorization rate can reach 67%, mainly because not only new impurity levels is generated at the top of the valence band, but also the position of the bottom of the conduction band decreases more, making the band gap of the SDBS/C/Nd/TiO<sub>2</sub> narrower, which was conducive to widening the photoabsorption range of the catalyst, thus improving the photocatalytic performance of the SDBS/C/Nd/TiO<sub>2</sub> catalyst.

#### Acknowledgements

This paper was supported by Tianjin Science and Technology Plan Project (21YFSNSN00240).

#### References

- Chen F.J., Ho P.L., Ran R., Chen W.M., Si Z.C., Wu X.D., Weng D., Huang Z.H. and Lee C.Y. (2017). Synergistic effect of CeO<sub>2</sub> modified TiO<sub>2</sub> photocatalyst on the enhancement of visible light photocatalytic performance, *Journal of Alloys and Compounds*, **714**, 560–566.
- Chen X.B., Shen S.H., Guo L.J. and Mao S.S. (2010). Semiconductor-based Photocatalytic Hydrogen Generation, *Chemical Reviews*, **110**, 6503–6570.
- Dwiyanna R., Roto R., Suwondo K.P. and Wahyuni E.T. (2021). Enhanced photocatalytic degradation of Remazol Black under visible light illumination through S doped TiO<sub>2</sub> (S-TiO<sub>2</sub>) nanoparticles: Operational factors and kinetic study, *Global NEST Journal*, **23**, 323–332.
- Jin Y.L., Wang J.Y., Gao X., Ren F., Chen Z.Y., Sun Z.F. and Ren P.G. (2023). Spent Coffee Grounds Derived Carbon Loading C, N Doped TiO<sub>2</sub> for Photocatalytic Degradation of Organic Dyes, *Materials*, **16**, 5137–5150.
- Kader S., Al-Mamun M.R., Suhan M.B.K., Shuchi S.B. and Islam M.S. (2022). Enhanced photodegradation of methyl orange dye under UV irradiation using MoO<sub>3</sub> and Ag doped TiO<sub>2</sub>

- photocatalysts, *Environmental Technology & Innovation*, **27**, 102476–102490.
- Krylov I.B., Lopat'eva E.R., Subbotina I.R., Nikishin G.I., Yu B. and Terent'ev A.O. (2021). Mixed hetero-/homogeneous TiO<sub>2</sub>/N-hydroxyimide photocatalysis in visible-light-induced controllable benzylic oxidation by molecular oxygen, *Chinese Journal of Catalysis*, **42**, 1700–1711.
- Kuerbanjiang B., Wiedwald U., Hirling F., Biskupek J., Kaiser U., Ziemann P. and Herr U. (2013). Exchange bias of Ni nanoparticles embedded in an antiferromagnetic IrMn matrix, *Nanotechnology*, **24**, 455702–455710.
- Kunarti E.S., Roto R., Nuryono N., Santosa S.J. and Fajri M.L. (2020). Photocatalytic Reduction of AuCl<sub>4</sub><sup>-</sup> by Fe<sub>3</sub>O<sub>4</sub>/SiO<sub>2</sub>/TiO<sub>2</sub> Nanoparticles, *Global NEST Journal*, **22**, 119–125.
- Li H., Hao Y., Lu H., Liang L., Wang Y., Qiu J., Shi X., Wang Y. and Yao J. (2015). A systematic study on visible-light N-doped TiO<sub>2</sub> photocatalyst obtained from ethylenediamine by sol-gel method, *Applied Surface Science*, **344**, 112–118.
- Liu R.Y., Hu P.G. and Chen S.W. (2012). Photocatalytic activity of Ag<sub>3</sub>PO<sub>4</sub> nanoparticle/TiO<sub>2</sub> nanobelt heterostructures, *Applied Surface Science*, **258**, 9805–9809.
- Marzec A., Radecka M., Maziarz W., Kusior A. and Pędzich Z. (2016). Structural, optical and electrical properties of nanocrystalline TiO<sub>2</sub>, SnO<sub>2</sub> and their composites obtained by the sol-gel method, *Journal of the European Ceramic Society*, **36**, 2981–2989.
- Rengaraj S., Venkataraj S., Yeon J.W., Kim Y.H., Li X.Z. and Pang G.K.H. (2007). Preparation, characterization and application of Nd-TiO<sub>2</sub> photocatalyst for the reduction of Cr(VI) under UV light illumination, *Applied Catalysis B: Environmental*, **77**, 157–165.
- Si Y.J., Liu H.H., Li N.T., Zhong J.B., Li J.Z. and Ma D.M. (2018). SDBS-assisted hydrothermal treatment of TiO<sub>2</sub> with improved photocatalytic activity, *Materials Letters*, **212**, 147–150.
- Sirivallop A., Areerob T. and Chiarakorn S. (2020). Enhanced Visible Light Photocatalytic Activity of N and Ag Doped and Co-Doped TiO<sub>2</sub> Synthesized by Using an In-Situ Solvothermal Method for Gas Phase Ammonia Removal, *Catalysts*, **10**, 251–268.
- Sudarsanam P., Li H. and Sagar T.V. (2020). TiO<sub>2</sub>-Based Water-Tolerant Acid Catalysis for Biomass-Based Fuels and Chemicals, *ACS Catalysis*, **10**, 9555–9584.
- Verbruggen S.W. (2015). TiO<sub>2</sub> photocatalysis for the degradation of pollutants in gas phase: From morphological design to plasmonic enhancement, *Journal of Photochemistry and Photobiology C: Photochemistry Reviews*, **24**, 64–82.
- Vishwakarma M.K., Bag M. and Jain P. (2023). Metal and Nonmetal Ion Doping Effect on the Dielectric Relaxation of TiO<sub>2</sub> Electrodes, *Physica Status Solidi A-Applications and Materials Science*, **220**, 2200807-.
- Wang J.C., Qiao X., Shi W.N., Gao H.L. and Guo L.C. (2022). Enhanced Photothermal Selective Conversion of CO<sub>2</sub> to CH<sub>4</sub> in Water Vapor over Rod-Like Cu and N Co-Doped TiO<sub>2</sub>, *Chinese Journal of Structural Chemistry*, **41**, 2212033–2212042.
- Xia J., Dong L.Z., Song H.Y., Yang J. and Zhu X.S. (2023). Preparation of doped TiO<sub>2</sub> nanomaterials and their applications in photocatalysis, *Bulletin of Materials Science*, **46**, 13–28.

- Xiao J.D., Xie Y.B., Cao H.B., Nawaz F., Zhang S.S. and Wang Y.Q. (2016). Disparate roles of doped metal ions in promoting surface oxidation of TiO<sub>2</sub> photocatalysis, *Journal of Photochemistry and Photobiology A: Chemistry*, **315**, 59–66.
- Xie F.X., Cherng S.J., Lu S.M., Chang Y.H., Sha W.E.I., Feng S.P., Chen C.M. and Choy W.C.H. (2014). Functions of Self-Assembled Ultrafine TiO<sub>2</sub> Nanocrystals for High Efficient Dye-Sensitized Solar Cells, *ACS Applied Materials & Interfaces*, **6**, 5367–5373.
- Yin S., Aita Y., Komatsu M., Wang J., Tang Q. and Sato T. (2005). Synthesis of excellent visible-light responsive TiO<sub>2-x</sub>N<sub>y</sub> photocatalyst by a homogeneous precipitation-solvothermal process, *Journal of Materials Chemistry*, **15**, 674–682.
- Yu A., Wang Q.J., Wang J.J. and Chang C.T. (2017). Rapid synthesis of colloidal silver triangular nanoprisms and their promotion of TiO<sub>2</sub> photocatalysis on methylene blue under visible light, *Catalysis Communications*, **90**, 75–78.
- Zhang T.T., Li H., Tang X.Q., Zhong J.B., Li J.Z., Zhang S.L., Huang S.T. and Dou L. (2023). Boosted photocatalytic performance of OVs-rich BiVO<sub>4</sub> hollow microsphere self-assembled with the assistance of SDBS, *Journal of Colloid and Interface Science*, **634**, 874–886.
- Zhao J.W., Wang B., Zhao Y.R., Hou M.M., Xin C.H., Li Q. and Yu X. (2023). High-performance visible-light photocatalysis induced by dye-sensitized Ti<sup>3+</sup>-TiO<sub>2</sub> microspheres, *Journal of Physics and Chemistry of Solids*, **179**, 111374–111378.